479

KINEMATICS AND AERODYNAMICS OF THE GREATER HORSESHOE BAT, *RHINOLOPHUS FERRUMEQUINUM*, IN HORIZONTAL FLIGHT AT VARIOUS FLIGHT SPEEDS

BY H. D. J. N. ALDRIDGE*

Department of Zoology, University of Bristol, Woodland Road, Bristol BS8 1UG, UK

SUMMARY

The kinematics and aerodynamics of the greater horseshoe bat, *Rhinolophus ferrumequinum*, in horizontal flight at a range of velocities are described. As flight speed increases there is a gradual change in the bat's wingbeat kinematics, wingbeat frequency decreasing and wingbeat strokeplane angles increasing. Associated with these changes are changes in the wings' incidence angles, particularly during the upstroke. At low speeds these are large and negative, suggesting thrust generation, while at high speeds these are positive and large, indicating that weight support and negative thrust are being generated. The change from one kinematic pattern to the other occurred gradually. The possible energetic and aerodynamic reasons for these changes are discussed.

INTRODUCTION

A gliding animal loses height because the wings generate a vertical force which supports the animal's weight, but does not counteract drag – the sum of wing friction (profile drag), body friction (parasite drag) and the drag associated with wake vortex formation (induced drag). By flapping its wings the animal alters the direction of the force generated so that drag is counteracted and level flight sustained. As flight speed increases the relative magnitudes of the three drag components change, the relationship between flight speed and total drag taking the form of a U-shaped curve (Pennycuick, 1975). To sustain level flight at a range of speeds, the animal must alter its wingbeat kinematics so that thrust generated equals drag at all speeds.

In *Columba livia* the changes from one kinematic pattern to another appear to occur gradually in response to the gradual changes in the magnitudes of drag (Brown, 1948, 1953; Pennycuick, 1968). In flight immediately after take-off, the bird uses a 'tip-reversal' upstroke during which the primary feather region of the wing generates both weight support and thrust, only weight support being generated during the downstroke (Brown, 1948). When flying very slowly the secondary feather region is probably not moving fast enough to generate any useful aerodynamic forces (Boel,

---

* Present address: Department of Biology, York University, 4700 Keele Street, Downsview, M3J 1P3, Ontario, Canada.

Key words: bat, flight.

1929; Brown, 1948). This type of upstroke has also been reported in bats, although it was thought that the upstroke force is essentially horizontal, taking the form of supplementary thrust (Eisentraut, 1936; Norberg, 1976; Altenbach, 1979; Aldridge, 1985a). At higher speeds *C. livia* uses a 'feathered' upstroke, where the wing is brought close to the body, with the primary feathers rotated so that they present a 'Venetian blind' appearance to the oncoming air. The wing is only active during the downstroke, the bird's wake taking the form of a series of small-cored vortex rings (Kokshaysky, 1979; Spedding, Rayner & Pennycuick, 1984). This type of upstroke has not been described in bats and it has been suggested that this is because bats are unable to slot the handwing membrane (Aldridge, 1985b), although by maintaining incidence angles at or around zero during the upstroke the noctule *Nyctalus noctula* generates the same type of wake (Rayner, 1986). As the pigeon's flight speed approaches normal commuting speeds the flight kinematics change again; the wing remains partially extended during the upstroke and force is generated throughout the wingstroke (Brown, 1948). The kestrel, *Falco tinnunculus*, and *N. noctula* both use this type of upstroke (the so-called 'reduced span') in cruising flight, force being generated as a result of the generation of a pair of distorted parallel vortices (Spedding, 1981).

The purpose of this paper is to address two questions concerning the flight of *R. ferrumequinum*. (i) What are the kinematic and aerodynamic changes accompanying increases in flight speed and (ii) are these changes gradual or do they occur abruptly?

MATERIALS AND METHODS

Husbandry

Two male *R. ferrumequinum* were obtained and kept in captivity for 18 months. They were housed in a plywood box (0·6 m × 0·6 m × 0·6 m), the walls of which were lined with non-toxic plastic netting. In the bottom of the box there was an aluminium tray lined with moist paper towelling which ensured that the relative humidity did not fall below 80 %. The temperature in the animal room followed ambient unless it dropped below 10°C, when supplementary electric heating was automatically turned on. This ensured that the bats could enter torpor regularly but did not go into hibernation. The bats were fed on a diet of mealworm larvae (*Tenebrio molitor*), occasionally supplemented by insects caught in a mercury-vapour light trap. A vitamin supplement (Vionate) was added to the bran in which the mealworms were kept and sprinkled sparingly over the food before presentation. Water was always available, the bats quickly learning to drink from a normal small mammal water bottle.

Training

One bat was trained to fly through a flight tunnel on the execution of an auditory command (the clicking of my fingers). When the bats were first brought into captivity they had to be restrained when being fed or watered. After a few weeks they

Table 1. *Morphological parameters for* Rhinolophus ferrumequinum

Mass (kg)	0·022
Span (m)	0·360
Area (m^2)	0·022
Wingloading (N m^{-2})	9·5
Aspect ratio	5·8

could be fed without restraint, but had to be captured (with a hand-net) and placed upon the feeding perch before they would take food. By this stage they had learnt to take water from a small mammal water bottle suspended in their box. Presentation of food was always accompanied by the auditory signal, and eventually both bats would respond by flying towards it. Only one, however, would land on the feeding perch, the other catching mealworms thrown into the air. The bat which landed on the feeding perch could be handled with ease, and it was this individual that was used for the experiments. The bat's morphological parameters are presented in Table 1. Experiments were only carried out before the bat was fed, thereby ensuring that the bat was alert to the auditory signal. By clicking my fingers I could call the bat to the feeding perch and from there it could be carried to the flight tunnel where it was placed on a second perch and given a small mealworm fragment. After eating the fragment the bat would normally stay hanging from the perch grooming. By repeating the auditory signal the bat could be induced to fly through the tunnel to the feeding perch, where it was rewarded with another mealworm fragment; the procedure could then be repeated. The bat could be used in experiments for long periods without a noticeable decrease in performance or alertness, as long as only small pieces of mealworm were given as reward.

Photography

The photographic technique used by Rayner & Aldridge (1985) to analyse the turning flight of *Plecotus auritus* was also used in this study. The bat flew through the flight tunnel, triggering the two cameras (Nikon FM plus MD11 motordrive and Nikon FM2 plus MD12 motordrive, both with Nikkor 55 mm Micro lenses) by interrupting a light beam. The two cameras were arranged on mutually perpendicular axes (the FM suspended above the flight tunnel, the FM2 to one side) (Rayner & Aldridge, 1985). The camera shutters were set to open for up to 1 s while the bat flew through the tunnel, illuminated by a stroboscope (Dawe Instruments 1203c 'Strobosun') flashing at 100 or 200 Hz. A series of cotton threads was arranged within the flight tunnel so that they defined the corners of a 0·4 m cube (Rayner & Aldridge, 1985). The threads were permanently arranged, and therefore appeared in every pair of photographs. For each flight two multi-image photographs were produced, one showing the dorsal view, the other the lateral view of the bat's flight path through the tunnel. The data were put into a Research Machines 380Z microcomputer through a Summagraphics Bit-Pad One digitizing tablet.

Analysis

Kinematic measurements

For each flight the positions, in three dimensions, of the body (represented by the eye in the photograph showing the lateral view and a point midway between the ears on the photograph showing the dorsal view), the wrist, the tips of the second, fourth and fifth digits and the wingtip (tip of the third digit) (Fig. 1) were obtained by resection for a sequential series of images (Rayner & Aldridge, 1985). From these data five kinematic parameters were calculated: flight velocity (V), wingbeat frequency (f), wingbeat amplitude (θ) and the strokeplane angles for the wrist (γ_w) and the wingtip (γ_{wt}). The velocities of the wrist, wingtip, second, fourth and fifth digits were calculated as described by Rayner & Aldridge (1985), total wingtip velocity (V_t) being defined as:

$$V_t = \sqrt{v_x^2 + v_y^2 + v_z^2}, \tag{1}$$

where v_x^2, v_y^2 and v_z^2 are wingtip velocities in the forward, lateral and vertical directions, respectively.
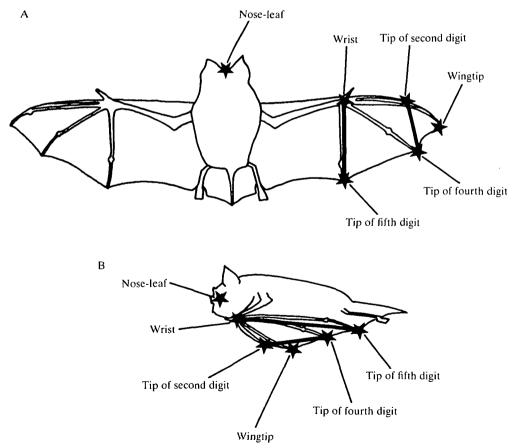

Fig. 1. The positions of the wrist, the tip of the second, fourth and fifth digits and the wingtip as seen from above (A) and from the side (B). The positions of the two wing-chords are also shown.

Wingbeat frequency was calculated by counting the number of images over a whole wingbeat, starting and finishing at the beginning of the downstroke. Wingbeat amplitude is here defined as the angle moved during the downstroke by the proximal portion of the wing (defined as a line drawn between the point representing the body and the wrist) (Pennycuick, 1968). The movement of the wing during the downstroke can be approximated to movement in a single plane, and is defined by a line drawn between wing position at the beginning and end of the downstroke (Pennycuick, 1968). The strokeplane angle is the angle between this plane and the horizontal. In this study two estimates of strokeplane angle were calculated, for the wrist and the wingtip (Scholey, 1982).

The accuracy of these measurements is determined by the accuracy of test cube construction, optical distortion, digitizing errors and difficulties in determining image locations on the photographs. Rayner & Aldridge (1985) have estimated the maximum possible error in point position estimation as being between 2 and 4% of any linear distance, as long as the cameras are positioned not more than 10° away from the ideal camera axes (Rayner & Aldridge, 1985). In practice it was found that a test cube was relatively easy to construct accurately and by using a spirit level or a plumb line the cameras could be arranged with tilt angles of less than 5°.

The absolute accuracy with which the kinematic parameters can be determined is dependent upon the frequency of sampling. Ideally the interval between images should be as small as possible so that rapid changes of position or speed can be resolved. A limit was set on this interval by (1) the quantity of light delivered in each flash, which falls as frequency is increased, and (2) the need for each overlapping image to be distinguished. The maximum practical flash rate was found to be 100 Hz although in some cases 200 Hz could satisfactorily be used (the higher the flight speed, the higher the frequency had to be to produce enough images for analysis). Aldridge (1985a) recorded maximum wingtip speeds in *R. ferrumequinum* of approx. $13 \, \text{m s}^{-1}$, and at these high speeds the wingtip could move as much as 13 mm between consecutive flashes. Fortunately the mean wing speed is lower than this (approx. $5 \, \text{m s}^{-1}$) but at critical stages during the wingbeat, such as the beginning and end of the downstroke, the discrepancy between the estimated positions of the wingtip and wrist and their true positions may be as much as 4%. This source of error will be most noticeable in the estimates of wingbeat amplitude.

Wingchord angles

An indication of wing function can be obtained from estimates of the changes in incidence angles at regular stages during the wingbeat cycle. A wingchord is defined here as being a straight line between two points on the leading and trailing edges of the wing, respectively. For this investigation two wingchords were used, the wrist chord, a line drawn between the wrist and the tip of the fifth digit, and the wingtip chord drawn between the tips of the second and fourth digits (Fig. 1) (Norberg, 1976). The positions, in three dimensions, of the two wingchords were calculated at regular intervals, and the angles of incidence for both chords were calculated by determining the local velocity vectors of the two ends of the chords, and finding the
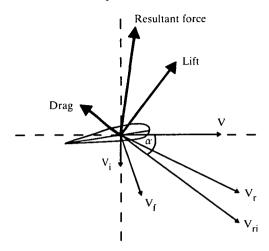
Fig. 2. Local velocity and force vectors at a wingchord in horizontal flight. V_{ri} is the resultant of the animal's flight speed, V, flapping velocity, V_f, and induced velocity V_i, while V_r is the resultant of V and V_f. The angle (the angle of incidence) between V_{ri} and the wingchord is α.

angle between the chord and a line parallel to the mean of the two velocities by vector methods.

The relative airflow (V_{ri}) is the resultant of the bat's forward speed (V), the wing's flapping velocity (V_f) and the induced velocity (V_i) (Fig. 2). Induced velocity is the vector sum of bound and wake vorticities which, without techniques which either visualize or measure airflows around flying animals (e.g. Kokshaysky, 1979; Spedding *et al.* 1984), are difficult to estimate. Using the Rankine–Froude momentum theory of propellers it is possible to obtain an estimate of mean vertical induced velocity. V_i can be defined by the formula:

$$V_i = W/2VS_d\rho \qquad (2)$$

where W is the bat's mass, S_d is wing disk area and ρ is air density (Pennycuick, 1975). Equation 2 assumes that V_i is constant across the wingspan, and throughout the wingbeat.

At high flight speeds the resultant airflow is dominated by V and the effect of V_i is probably negligible, and for this reason V_i was ignored in my estimations of incidence angles. As flight speed decreases, wake-induced velocity reaches a maximum and V_i

Table 2. *Kinematic parameters for* Rhinolophus ferrumequinum *flying at* $2\cdot7\,m\,s^{-1}$, $3\cdot1\,m\,s^{-1}$ *and* $4\cdot8\,m\,s^{-1}$

V ($m\,s^{-1}$)	f (Hz)	θ (degrees)	γ_w (degrees)	γ_{wt} (degrees)	V_i ($m\,s^{-1}$)
2·7	13·0	90·0	88·0	74·0	0·39
3·1	11·1	65·0	83·0	67·5	0·27
4·8	9·1	64·0	90·0	85·0	0·22

Abbreviations are explained in the Appendix.

becomes increasingly unreliable. In hovering animals, when wake-induced velocity is highest, the bound vorticity of one wing is likely to affect that of the other, thus altering the direction and magnitude of the instantaneous induced velocity and making the discrepancy between estimates of V_i and their true values very large (Ellington, 1984a). In this situation the estimates of incidence angles obtained are likely to be very inaccurate, and therefore result in serious error in the estimation of the direction and magnitude of the forces generated. Assuming that the ratio between mean induced velocity and forward speed is likely to be highest in a slow-flying bat, I estimated V_i for *R. ferrumequinum* flying at $2 \cdot 7 \, \mathrm{m \, s}^{-1}$ and calculated incidence angles with and without this value, to see whether mean induced velocity had a significant effect on it.

RESULTS

The effect of V_i

Using equation 2, values of V_i for *R. ferrumequinum* flying at $2 \cdot 7 \, \mathrm{m \, s}^{-1}$, $3 \cdot 1 \, \mathrm{m \, s}^{-1}$ and $4 \cdot 8 \, \mathrm{m \, s}^{-1}$ were calculated and the results are presented in Table 2. In Fig. 3 the
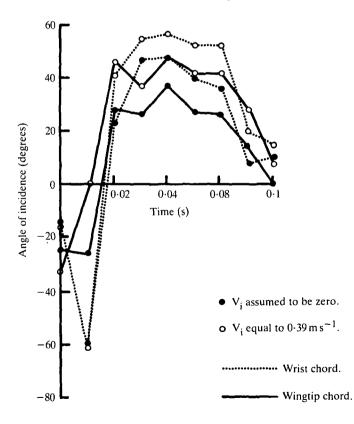

Fig. 3. Changes in the angles of incidence for the wrist and wingtip chords in *Rhinolophus ferrumequinum* flying at $2 \cdot 7 \, \mathrm{m \, s}^{-1}$, with V_i assumed to be zero (solid circles) and V_i set to $0 \cdot 39 \, \mathrm{m \, s}^{-1}$ (open circles).
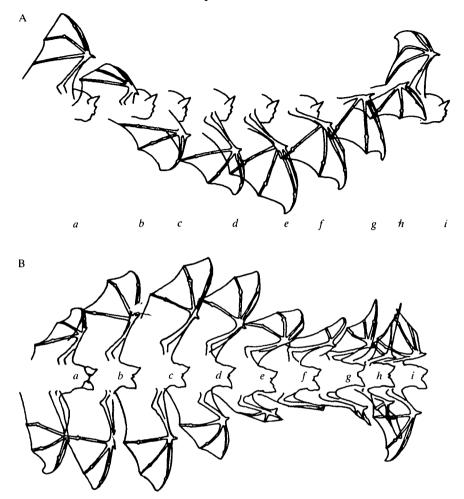
A

B

Fig. 4. Drawings of *Rhinolophus ferrumequinum* in horizontal flight at $2.7 \, \text{m s}^{-1}$ taken from multiflash photographs (stroboscope flash frequency 100 Hz); (A) lateral view; (B) dorsal view.

angles of incidence for *R. ferrumequinum* flying at $2.7 \, \text{m s}^{-1}$ for V_r (calculated without an estimate of V_i) and V_{ri} (calculated with $V_i = 0.39 \, \text{m s}^{-1}$) are plotted.

Wingbeat kinematics

When flying at $2.7 \, \text{m s}^{-1}$ the downstroke is initiated with the wing fully extended, and held at an angle of 54° above the horizontal (Fig. 4A). The wing is accelerated forwards and downwards reaching a maximum wingtip downstroke speed of $6.9 \, \text{m s}^{-1}$ midway through the downstroke (Figs 6, 9). When the proximal portion of the wing reaches 36° below the horizontal, it begins to rise, the wingtip continuing to move downwards and forwards for a further $0.01 \, \text{s}$. Flexion of the wrist at this point accelerates the wing inwards; overall wingtip speed is, however, falling (Fig. 9). Midway through the downstroke incidence angles become positive and high (Fig. 12). After a further $0.02 \, \text{s}$ the wing begins to decelerate (Fig. 9), and the
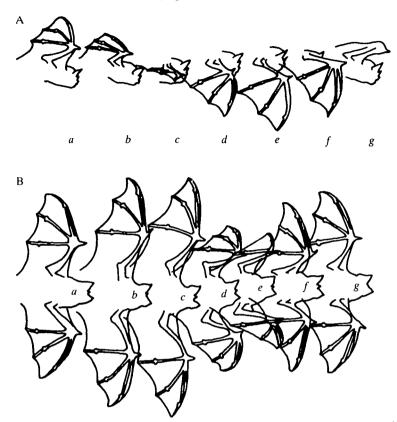
Fig. 5. Drawings of *Rhinolophus ferrumequinum* in horizontal flight at 4·8 m s⁻¹ taken from multiflash photographs (stroboscope flash frequency 100 Hz); (A) lateral view; (B) dorsal view.

incidence angles begin to fall (Fig. 12). The upstroke starts with the elbow and wrist fully flexed and the digits fully extended (Fig. 4*f*). As the upstroke proceeds the elbow and wrist extend, and as a result the handwing is extended perpendicular to the long axis of the body (Fig. 4*g–h*). This movement is accomplished rapidly as the wing is accelerated upwards and backwards (Fig. 9), the angles of incidence becoming momentarily negative and large (Fig. 12).

At 3·1 m s⁻¹ the bat moves its wings in essentially the same manner. There are, however, a number of significant differences. The upward and backward movement of the wing during the upstroke is reduced (Fig. 7) and there is no dramatic upstroke acceleration of the wingtip (Fig. 10). The angles of incidence are lower during the downstroke, and do not become large during the upstroke (Fig. 12).

The changes observed at 3·1 m s⁻¹ are more noticeable at 4·8 m s⁻¹. The backward movement of the wing during the upstroke is now totally lost, and the strokeplane becomes vertical (Fig. 8). The angles of incidence during the upstroke are large and positive (Fig. 12). There is no marked upstroke acceleration, wingtip speed remaining almost constant throughout the wingbeat (Fig. 11). At the beginning of the downstroke the wing is not fully extended, extending during the first half-stroke

(Fig. 5a–c). The wing remains partially extended during the upstroke and, as seen from above, the wingchords appear almost parallel to the long axis of the body (Fig. 5e–g).
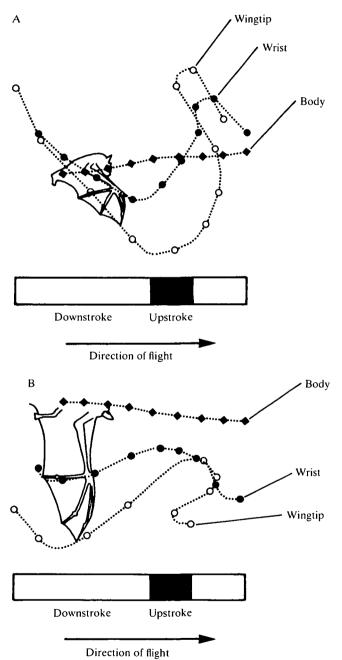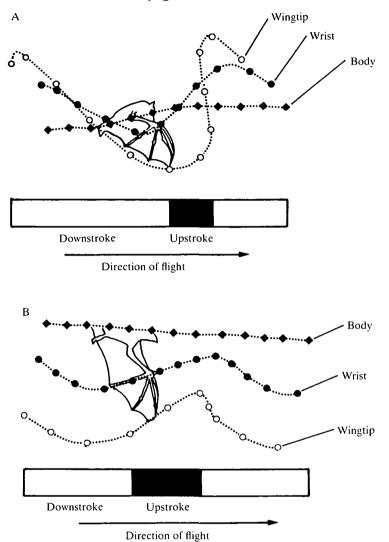

Fig. 6. Movements of the wrist, wingtip and body relative to the air in *Rhinolophus ferrumequinum* flying at $2.7 \, \mathrm{m \, s^{-1}}$; (A) lateral projection; (B) dorsal projection. Symbols are separated by $0.01 \, \mathrm{s}$.

Fig. 7. Movements of the wrist, wingtip and body relative to the air in *Rhinolophus ferrumequinum* flying at $3 \cdot 1 \, \mathrm{m \, s^{-1}}$; (A) lateral projection; (B) dorsal projection. Symbols are separated by $0 \cdot 01$ s.

As the bat's flight speed increases there is a significant, but small, fall in its wingbeat frequency ($b = -0 \cdot 71$, $r = -0 \cdot 39$, $P < 0 \cdot 01$) (Fig. 13A), and a significant increase in wing strokeplane angles ($b = 3 \cdot 5$, $r = 0 \cdot 33$, $P < 0 \cdot 01$ for the wrist and $b = 5 \cdot 71$, $r = 0 \cdot 33$, $P < 0 \cdot 01$ for the wingtip) (Fig. 14). There is no significant difference between the slopes of the two regression lines ($F = 2 \cdot 2$, $P > 0 \cdot 05$). There is no significant correlation between wingbeat amplitude and flight speed ($r = -0 \cdot 05$, $P > 0 \cdot 05$) (Fig. 13B), although there is a tendency for amplitude to be lower at higher speeds (Table 2). As discussed above, of all the kinematic parameters, amplitude is probably the most sensitive to errors in pinpointing the exact beginning

and end of the downstroke, and this may be the reason for there being no significant trend.

DISCUSSION

A flying animal flaps its wings primarily to generate thrust; if circulation is kept constant throughout the wingbeat no net thrust will be generated, the forces generated during the up- and downstrokes having equal magnitude but opposite sign. To generate net thrust it is essential that there is asymmetry between the up-
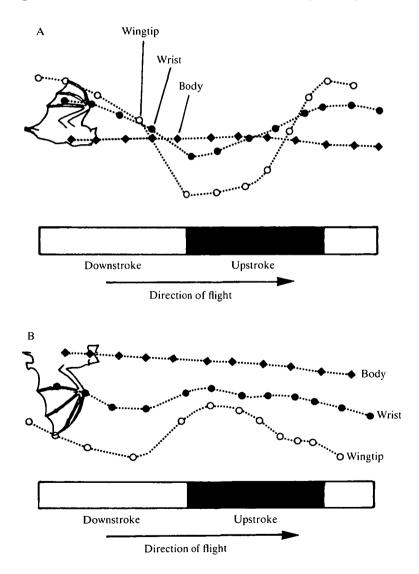

Fig. 8. Movements of the wrist, wingtip and body relative to the air in *Rhinolophus ferrumequinum* flying at $4 \cdot 8 \, \text{m s}^{-1}$; (A) lateral projection; (B) dorsal projection. Symbols are separated by $0 \cdot 01 \, \text{s}$.

and downstrokes. By changing either incidence angles or wing planform geometry, the animal can reduce the magnitude of upstroke thrust and therefore achieve wingbeat asymmetry. At low and high speeds [speeds below minimum power speed
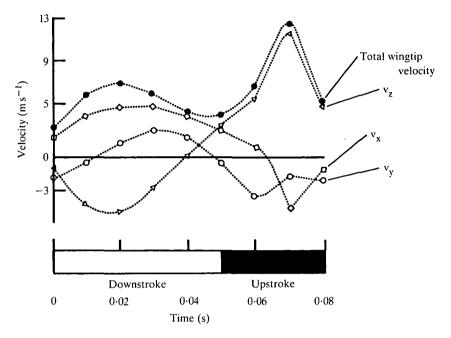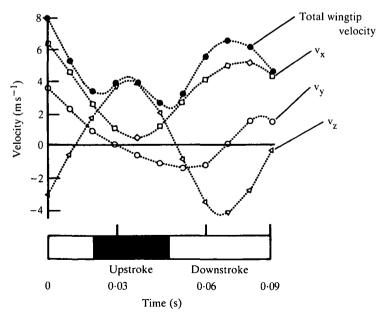

Fig. 9. Changes in the wingtip velocity in three dimensions (v_x, v_y and v_z) and total wingtip velocity in *Rhinolophus ferrumequinum* flying at $2 \cdot 7 \, \mathrm{m s^{-1}}$.

Fig. 10. Changes in the wingtip velocity in three dimensions (v_x, v_y and v_z) and total wingtip velocity in *Rhinolophus ferrumequinum* flying at $3 \cdot 1 \, \mathrm{m s^{-1}}$.
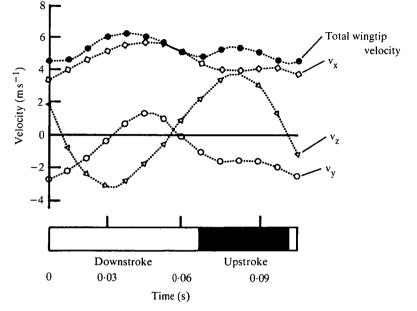
Fig. 11. Changes in the wingtip velocity in three dimensions (v_x, v_y and v_z) and total wingtip velocity in *Rhinolophus ferrumequinum* flying at $4.8\,\mathrm{m\,s^{-1}}$.
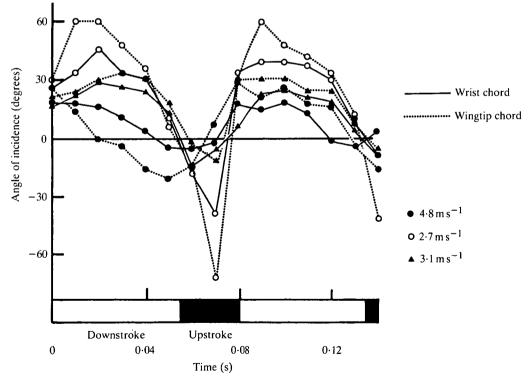

Fig. 12. Changes in the angles of incidence for the wrist and wingtip chords in *Rhinolophus ferrumequinum* flying at $2.7\,\mathrm{m\,s^{-1}}$, $3.1\,\mathrm{m\,s^{-1}}$ and $4.8\,\mathrm{m\,s^{-1}}$.

(V_{mp}) and above maximum range speed (V_{mr})], when drag is high, upstroke wing angles of incidence should be low and no force should be generated (Rayner, 1986). At intermediate speeds, when total drag is low, the upstroke could be used to generate weight support, net thrust ensured by the reduction of wing planform geometry. The fact that the changes in drag are gradual suggests that there should also be a gradual change in upstroke function as flight speed increases.

When flying at $2·7\,\mathrm{m\,s}^{-1}$ *R. ferrumequinum* uses a 'tip-reversal' upstroke; the proximal region of the wing is highly flexed with wristchord angles of incidence remaining low, suggesting that no aerodynamic work is being done; the digits are extended into the airstream and wingtip chord angles of incidence become momentarily large and negative, suggesting that a large propulsive force is being generated. Theoretically at low flight speeds the upstroke should be inactive, because induced drag is high (Rayner, 1986). However, Brown (1948) points out that because the wing is moving in the opposite direction to the body, drag will tend to propel the animal forward. Also the bat may have to generate a propulsive force during the upstroke because the force generated during the downstroke is not large
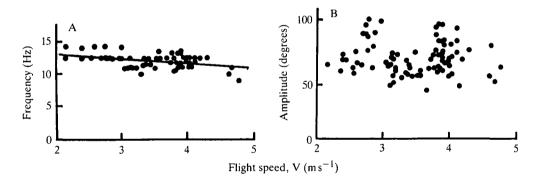

Fig. 13. Flight speed plotted against wingbeat frequency (A) and wingbeat amplitude (B) for *Rhinolophus ferrumequinum* in horizontal flight.
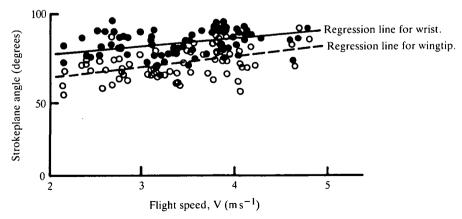

Fig. 14. Flight speed plotted against wrist and wingtip strokeplane angles for *Rhinolophus ferrumequinum* in horizontal flight.

enough to counteract drag, only the wingtip region of the wing generating any lift (Boel, 1929).

Brown (1948) predicted and confirmed (Brown, 1953) that as the pigeon's flight speed increased two processes should occur; (1) the backward 'flick' of the wingtip should be reduced and (2) there should be a transfer of lift generation to the downstroke. This sequence was also observed in *R. ferrumequinum*. When flying at $3·1 \, m \, s^{-1}$ *R. ferrumequinum* uses a 'feathered' upstroke, during which no force is generated. Presumably the increase in the wings' speed during the downstroke increases the force generated, and as a result reduces the need for upstroke thrust generation. At this speed (above V_{mp}) induced drag is still high and therefore no advantage would be gained by upstroke lift generation.

The minimum power speed (V_{mp}) for the individual used in this study is $4·84 \, m \, s^{-1}$. When flying at this speed the total drag on the bat will be minimal. The upstoke is therefore used to generate a backward- and upward-directed force, net thrust being ensured by upstroke wingspan reduction. The advantage of this kinematic pattern is that by generating lift over the whole wingbeat cycle the bat can reduce downstroke wing angular velocity and therefore flight muscle power output.

As the bat's flight speed increases there is a significant decrease in wingbeat frequency and an indication of a similar decrease in amplitude, which will result in a decrease in flight muscle power output. Presumably the increase in flight velocity and the decrease in drag enable the bat to reduce flight costs while ensuring that weight is supported and drag counteracted. The fact that wingbeat frequency changes with speed suggests that the flight muscles of *R. ferrumequinum* contain mixed fibre populations, similar to those found in *Hipposideros speoris* (George & Naik, 1957), because muscles consisting of a single fibre type should contract over a narrow frequency range to maximize efficiency (Goldspink, 1977).

The range of incidence angles at which a wing generates steady-state lift is determined by the wing's zero-lift angles and the angle at which steady-state stall occurs. As V increases the angle between V_{ri} and the horizontal decreases, assuming that V_f remains constant and unsteady phenomena are unimportant. The bat alters wing strokeplane angles to ensure that wingchord incidence angles remain between the zero-lift angle and the steady-state stall angle as the direction of V_{ri} changes. Fig. 12 shows that as the bat's flight speed increases there is a slight reduction in wingchord incidence angles, which may be a consequence of the lower thrust required as V approaches V_{mp}.

In calculating the incidence angles plotted in Fig. 12 it was assumed that V_i was negligible throughout the wingbeat and constant across wingspan. If the forces generated by the wings are produced by essentially steady-state phenomena, then it is probably safe to assume that V_i is constant; if, however, there is any unsteady flow V_i is likely to become momentarily very high, thus seriously affecting the airflow over the wings. Without some direct measurement of instantaneous airflow around the wings it is impossible to predict what these changes are and when in the wingbeat cycle they occur. But by calculating the advance ratio, J, we can estimate how

important unsteady flow might be. J measures the ratio of flapping velocity to mean flight velocity and is defined as:

$$J = V/2\gamma nR,\qquad(3)$$

where γ is strokeplane angle, n is wingchord length and R is wing length (Ellington, 1984*b*). High values of this parameter are associated with fast forward flight and are taken to indicate agreement with the quasi-steady assumption. The discrepancy between the value of V_i calculated from equation 2 and the true instantaneous value is likely to be most extreme when flight speed and the advance ratio are low and at points in the wingbeat cycle when there are high angles of rotation and high accelerations (Ellington, 1984*c*). Such are the conditions at the end of the upstroke and the beginning of the downstroke, particularly when the animal is flying slowly.

The advance ratios for *R. ferrumequinum* at $2 \cdot 7\,\mathrm{m\,s}^{-1}$, $3 \cdot 1\,\mathrm{m\,s}^{-1}$ and $4 \cdot 8\,\mathrm{m\,s}^{-1}$ are $0 \cdot 38$, $0 \cdot 54$ and $0 \cdot 93$, respectively. Although Norberg (1976) found that the flight of *P. auritus* flying at $2 \cdot 35\,\mathrm{m\,s}^{-1}$ ($J = 0 \cdot 5$) was explicable in steady-state terms, advance ratios below $0 \cdot 5$ are normally taken to indicate that unsteady effects are important. My interpretation of the directions of the forces generated by the wings during flight in *R. ferrumequinum* are likely only to be accurate at high speeds, when it is probably safe to assume that the wings are more or less functioning in accordance with the assumptions of steady-state aerodynamic theory, even though it has recently been shown that unsteady effects are probably also very important in fast forward flight (Clopeau, Devilliers & Devezeaux, 1979). At low speeds, when the advance ratio is large, the assumptions of the steady-state aerodynamic theory do not hold and therefore any estimates of incidence angles assuming steady-state conditions are likely to be very inaccurate because of unsteady airflow. For this reason it is not possible to say with confidence that the function of the upstroke in slow forward flight is the generation of thrust, because small inaccuracies in the estimates of the direction of the relative airflow during the upstroke might have implied negative angles of incidence, when in reality the angles are either near zero or even positive. Without some form of flow visualization or measurement it will not be possible to resolve this problem.

In conclusion, the results presented here indicate a gradual change in kinematics as the bat's flight speed increases up to V_{mp}. The changes observed are consistent with the hypothesis that upstroke function changes as drag decreases. Above V_{mp} drag increases again and further experiments are required to see whether, as predicted, the upstroke becomes inactive again.

APPENDIX

f	Wingbeat frequency	V	Flight velocity
J	Advance ratio	V_f	Velocity component due
m	Mass		to flapping
n	Wingchord length	V_i	Induced velocity
R	Wing length	V_r	Sum of V and V_f only

V_{mp}	Minimum power speed	S_d	Disk area
V_{mr}	Maximum range speed	α	Incidence angle
V_{ri}	Local relative air velocity	γ_w	Wrist strokeplane angle
V_t	Total wingtip velocity	γ_{wt}	Wingtip strokeplane angle
v_x	Forward component of V_f	θ	Wingbeat amplitude
v_y	Lateral component of V_f	ρ	Air density
v_z	Vertical component of V_f		

REFERENCES

ALDRIDGE, H. D. J. N. (1985a). The flight kinematics of the greater horseshoe bat (*Rhinolophus ferrumequinum*). In *Biona Report*, 5, *Fledermausflug* (ed. W. Nachtigall). Heidelberg: Gustav Fischer Verlag.

ALDRIDGE, H. D. J. N. (1985b). On the relationships between flight performance, morphology and ecology in British bats. Ph.D. thesis, University of Bristol.

ALTENBACH, J. S. (1979). Locomotor morphology of the vampire bat, *Desmodus rotundus. Spec. Publs. Am. Soc. Mammal.* 6, 75pp.

BOEL, M. (1929). Scientific studies of natural flight. *Trans. Am. Soc. mech. Engrs* 51, 217–242.

BROWN, R. H. J. (1948). The flight of birds. *J. exp. Biol.* 25, 322–333.

BROWN, R. H. J. (1953). The flight of birds. II. Wing function in relation to flight speed. *J. exp. Biol.* 30, 90–103.

CLOPEAU, M., DEVILLIERS, J. F. & DEVEZEAUX, D. (1979). Direct measurements of instantaneous lift in desert locust: comparison with Jensen's experiments on detached wings. *J. exp. Biol.* 80, 1–15.

EISENTRAUT, M. (1936). Beitrag zur Mechanik des Fledermausfluges. *Z. wiss. Zool.* 148, 159–188.

ELLINGTON, C. P. (1984a). The aerodynamics of hovering insect flight. The quasi-steady analysis. *Phil. Trans. R. Soc. Ser.* B 305, 1–14.

ELLINGTON, C. P. (1984b). The aerodynamics of hovering insect flight. III. Kinematics. *Phil. Trans. R. Soc. Ser.* B 305, 41–78.

ELLINGTON, C. P. (1984c). The aerodynamics of flapping animal flight. *Am. Zool.* 24, 95–104.

GEORGE, J. C. & NAIK, R. M. (1957). Studies on the structure and physiology of flight muscles of bats. I. The occurrence of two types of fibres in the pectoralis major muscle of the bat *Hipposideros speoris*, their relative distribution, nature of fuel store and mitochodrial content. *J. Anim. Morph. Physiol.* 4, 96–107.

GOLDSPINK, G. (1977). Mechanics and energetics of muscle in animals of different sizes, with particular reference to the muscle fibre composition of vertebrate muscle. In *Scale Effects in Animal Locomotion* (ed. T. J. Pedley). New York: Academic Press.

KOKSHAYSKY, N. V. (1979). Tracing the wake of a flying bird. *Nature, Lond.* 279, 146–148.

NORBERG, U. M. (1976). Aerodynamics, kinematics and energetics of horizontal flight in the long-eared bat *Plecotus auritus. J. exp. Biol.* 65, 179–212.

PENNYCUICK, C. J. (1968). Power requirements of flight for horizontal flight in the pigeon *Columba livia. J. exp. Biol.* 49, 527–555.

PENNYCUICK, C. J. (1975). Mechanics of flight. In *Avian Biology*, vol. 5 (ed. D. S. Farner, J. R. King & K. C. Parkes). London: Academic Press.

RAYNER, J. M. V. (1986). The mechanics of flapping flight in bats. In *Recent Advances in the Study of Bats* (ed. M. B. Fenton, P. A. Racey & J. M. V. Rayner). Cambridge: Cambridge University Press (in press).

RAYNER, J. M. V. & ALDRIDGE, H. D. J. N. (1985). Three-dimensional reconstruction of animal flight paths and the turning flight of microchiropteran bats. *J. exp. Biol.* **118**, 247–265.

SCHOLEY, K. D. (1982). Developments in vertebrate flight. Ph.D. thesis, University of Bristol.

SPEDDING, G. R. (1981). The vortex wake of flying birds: an experimental investigation. Ph.D. thesis, University of Bristol.

SPEDDING, G. R., RAYNER, J. M. V. & PENNYCUICK, C. J. (1984). Momentum and energy in the wake of the pigeon (*Columba livia*) in slow flight. *J. exp. Biol.* **111**, 81–102.